Two-photon transitions in systems with semiconductor quantum dots

A. V. Fedorov and A. V. Baranov
S. I. Vavilov State Optical Institute, 199034, St. Petersburg, Russia

K. Inoue
Research Institute for Electronic Science, Hokkaido University, Sapporo, 060, Japan
(Received 24 January 1996; revised manuscript received 16 April 1996)

Optical interband and intraband transitions in semiconductor quantum dots (QD's) are analyzed theoretically. It is found that three-dimensional confinement essentially modifies intraband matrix elements of the electron-photon interaction in the QD's as compared to the bulk materials. This effect is quite important for the multiphoton processes. It is shown that two competitive types of two-photon transitions with different selection rules are in the QD's of noncentrosymmetric semiconductor and amplitudes of these transitions differently depend on light polarization, electron and hole effective masses, and QD radius as well. Analytical expressions for the two-photon absorption coefficient are derived for the strong confinement regime, taking into account the size distribution of the nanocrystals. [S0163-1829(96)00235-4]

I. INTRODUCTION

Currently, the methods of nonlinear optics occupy an increasingly important place in experimental studies of nanocrystals, or quantum dots. Among studies of the nonlinear optical properties of such systems, experiments on two-photon absorption,[1] nonlinear bleaching,[2] four-photon mixing,[3] resonant hyper-Raman and hyper-Rayleigh scattering[4] should be mentioned. The interest in multiphoton processes in quantum dot (QD) systems is due to several reasons. Three-dimensional (3D) confinement drastically changes the electronic energy spectrum in nanocrystals as compared to the bulk material. Investigations of multiphoton processes, with selection rules and light polarization dependences different from those for one-photon processes, open up additional opportunities to study the unusual electronic structure of these systems in detail. The nonlinear optical properties of QD systems are themselves of interest, since the confinement essentially modifies the interaction of quasiparticles with electromagnetic field. Finally, investigations of multiphoton processes are promising for applications in optoelectronics. To our knowledge, despite the importance of the problem, a more or less adequate theoretical description of multiphoton effects in QD systems is not available.

In this paper, we theoretically analyze the effect of strong confinement[5] on optical interband and intraband transitions, as well as the two-photon generation rate (TPGR) of electron-hole pairs in QD's based on a direct-band semiconductor of symmetry O_h or T_d. These materials have a fairly simple structure of energy bands, and hence they are better model objects for experimental studies of 3D confinement than hexagonal semiconductors with strongly anisotropic and nonparabolic valence bands. The complex band structure of confinement systems is a severe problem in theoretical treatments of optical effects and the interpretation of experiments.

Analytical expressions for matrix elements of electron-photon interaction and the TPGR are derived in the effective-mass approximation for the well-known four-band model of the semiconductor,[6] explicitly including the doubly degenerate conduction band (c) and twofold degenerate bands of heavy (h_1), light (h_2), and spin-orbit-split (h_3) holes. It is assumed that electrons and holes are located in a spherical potential well of radius R with infinitely high walls, and that the Coulomb electron-hole correlation is negligibly small.

It is found that the intraband matrix elements are inversely proportional to the radius R and, thus, 3D confinement can significantly change the role of intraband and interband transitions in multiphoton processes as compared to the bulk semiconductors. It is shown that two competitive types of two-photon transitions with different selection rules are in QD's of noncentrosymmetric semiconductors, and that amplitudes of these transitions depend differently on light polarization, electron and hole effective masses, and QD radius as well. Finally, the two-photon absorption coefficient for the QD system was calculated with regard to the system's size distribution.

II. RATE OF TWO-PHOTON TRANSITIONS

The TPGR of electron-hole pairs by plane-polarized light with frequency ω can be represented in second-order perturbation theory with respect to the electron-photon interaction V as

$$W^{(2)}=\frac{2\pi}{\hbar}\sum_{\nu_1,\nu_0}|M_{\nu_1,\nu_0}|^2\delta(E_{\nu_1}-E_{\nu_0}-2\hbar\omega), \tag{1}$$

$$M_{\nu_1,\nu_0}=\sum_{\nu_2}\frac{V_{\nu_1,\nu_2}V_{\nu_2,\nu_0}}{E_{\nu_2}-E_{\nu_0}-\hbar\omega-i\hbar\gamma_{\nu_2}}. \tag{2}$$

In Eqs. (1) and (2), the subscripts ν_0, ν_1, and ν_2 denote sets of quantum numbers for initial, final, and intermediate states of an electron subsystem, respectively, and the parameter γ_ν is the inverse lifetime of the state ν. The composed matrix element Eq. (2) will be calculated in the effective-mass approximation for the four-band model of a cubic O_h or T_d semiconductor with an isotropic and parabolic electronic

spectrum. In addition, we assume that the potential of the QD has only diagonal matrix elements. In this case, under the condition of strong confinement, the electron wave function $\psi_\nu(\mathbf{x})$ is a product of the Bloch amplitude $\varphi_a(\mathbf{x})$ of the a band ($a=c$ or h_j) and the envelope wave function $\Psi_b(\mathbf{x})$ (Ref. 5) with composed index, $b=nlm$, where n, l, and m are the principal quantum number, the angular moment, and its projection, respectively. Hereafter, in order to simplify mathematical expressions, we will use yet another composed index, $\beta=nl$. With the above assumptions, the electron energy spectrum can be represented as

$$E_\beta^c=\frac{\hbar^2\xi_\beta^2}{2R^2m_c},\quad E_\beta^{h_j}=-E_{h_j}-\frac{\hbar^2\xi_\beta^2}{2R^2m_{h_j}}, \tag{3}$$

$$E_{h_1(h_2)}=E_g,\quad E_{h_3}=E_g+\Delta_{\mathrm{so}}, \tag{4}$$

where E_g and Δ_{so} are the energy gap and spin-orbit splitting in the bulk material, m_a is the effective mass in the a band, and $\xi_\beta=\xi_{n,l}$ is the nth root of the spherical Bessel function of lth order, $j_l(\xi_{n,l})=0$.

The **Ap** representation is used for the electron-photon interaction, where $\mathbf{A}=A\mathbf{e}$ is the vector potential of the light wave with amplitude A and the polarization vector $\mathbf{e}$, and $\mathbf{p}=-i\hbar\boldsymbol{\nabla}$ is the electron momentum operator. In what follows we assume that the semiconductor has T_d symmetry. All results are valid for the materials of O_h symmetry as well, unless otherwise specified.

Since in cubic semiconductors the one-photon interband transition $h_j\rightarrow c$, is allowed in the dipole approximation, each term in the sum [Eq. (2)] contains the product of the matrix elements $V_{c,b_1;h_j,b_0}$ and $V_{a,b_1;a,b_0}$ for one-photon transitions. Elements of the first type can be obtained immediately from the corresponding matrix elements for bulk material. To do this, it will suffice to call attention to the fact that the effect of 3D confinement is reduced to the substitution of the Kronecker symbol $\delta_{\mathbf{k}',\mathbf{k}}$, which expresses the momentum conservation law in one-photon interband transitions by the product of the Kronecker symbols $\delta_{n',n}\delta_{l',l}\delta_{m',m}$, arising from the orthogonality of the envelope wave functions. It is easily seen that, in the basis of coupled moments,[7] the matrix elements of the one-photon interband transitions are determined by the following expression:

$$\langle c,b'|V|h,b\rangle=i\delta_{n',n}\delta_{l',l}\delta_{m',m}\frac{P}{\sqrt{3}}\frac{eA}{\hbar c}\begin{pmatrix}\sqrt{3}e_{+1} & 0 & \sqrt{2}e_0 & e_{-1} & -e_0 & -\sqrt{2}e_{-1}\\ 0 & \sqrt{3}e_{-1} & e_{+1} & \sqrt{2}e_0 & \sqrt{2}e_{+1} & e_0\end{pmatrix}, \tag{5}$$

where $e_{\pm1}=\mp(e_x\pm ie_y)/\sqrt{2}$, $e_0=e_z$, e_j are the Cartesian components of the polarization vector ($j=x,y,z$), $P=\hbar p_{c,h}/m_0=\hbar^2\langle S|\partial/\partial z|Z\rangle/m_0$, m_0 is the free-electron mass, and $p_{c,h}$ is the interband matrix element of the electron momentum. In Eq. (5), the row numbering from top to bottom corresponds to the Bloch amplitudes $|c,\frac{1}{2},\frac{1}{2}\rangle$ and $|c,\frac{1}{2},-\frac{1}{2}\rangle$, and the column numbering from left to right corresponds to $|h_1,\frac{3}{2},\frac{3}{2}\rangle$, $|h_1,\frac{3}{2},-\frac{3}{2}\rangle$, $|h_2,\frac{3}{2},\frac{1}{2}\rangle$, $|h_2,\frac{3}{2},-\frac{1}{2}\rangle$, $|h_3,\frac{1}{2},\frac{1}{2}\rangle$, and $|h_3,\frac{1}{2},-\frac{1}{2}\rangle$. The first and second half-integer indices in the kets are equal to the total moment (i.e., a sum of angular and spin moments) and its projection. Thus, according to Eq. (5), the 3D confinement does not qualitatively change the electron-photon interaction in the case of interband transitions. Quite a different situation occurs in the case of intraband transitions whose matrix elements can be written as

$$\langle a,b'|V|a,b\rangle=-i\frac{e\hbar A}{cm_a}\frac{E_\beta^a}{|E_\beta^a|}\sum_{p=0,\pm1}(-1)^p e_p V_{b';b}^{(p)}, \tag{6}$$

where

$$V_{b';b}^{(p)}=-\frac{2}{R}\frac{\xi_{\beta'}\xi_\beta D_{b';b}^{(p)}}{(\xi_{\beta'}^2-\xi_\beta^2)\sqrt{(2l+1)(2l'+1)}}, \tag{7}$$

$$D_{b';b}^{(\pm1)}=\frac{\delta_{m',m\pm1}}{\sqrt{2}}[\delta_{l',l+1}\sqrt{(l'\pm m)(l\pm m+2)}-\delta_{l',l-1}\sqrt{(l'\mp m)(l\mp m)}],$$

$$D_{b';b}^{(0)}=\delta_{m',m}(\delta_{l',l+1}\sqrt{l'^2-m^2}-\delta_{l',l-1}\sqrt{l^2-m^2}). \tag{8}$$

From Eqs. (6)–(8), it follows that the 3D confinement essentially modifies the electron-photon interaction in this case as compared to the bulk material. Only off-diagonal matrix elements for this interaction are nonzero. In other words, no analogy with the momentum-conservation law exists for this interaction. Also, the intraband matrix elements depend explicitly upon the QD size, that is, the elements are inversely proportional to the radius R.

The TPGR of electron-hole pairs is readily calculated from Eqs. (5)–(8),

$$W^{(2)}=\frac{16\pi P^2}{9\hbar}\left(\frac{eA}{c}\right)^4[\tfrac{3}{2}(1-e_z^2)F_{c,h_1}+\tfrac{1}{2}(1+3e_z^2)F_{c,h_2}+F_{c,h_3}], \tag{9}$$

where the form functions for two-photon transitions from the valence band h_j to the conduction band c are given by

$$F_{c,h_j}=\frac{1}{R^2}\sum_{\beta_1,\beta_0}T_{\beta_1;\beta_0}^{c,h_j}\{l_1\delta_{l_1,l_0+1}+l_0\delta_{l_1,l_0-1}\}\times\frac{\xi_{\beta_1}^2\xi_{\beta_0}^2}{(\xi_{\beta_1}^2-\xi_{\beta_0}^2)^2}\delta(E_{\beta_1}^c-E_{\beta_0}^{h_j}-2\hbar\omega), \tag{10}$$

$$T^{c,h_j}_{\beta_1;\beta_0}=\left|\frac{1}{m_c}\frac{1}{E^c_{\beta_0}-E^c_{\beta_1}+\hbar\omega-i\hbar\gamma^c_{\beta_0}}+\frac{1}{m_{h_j}}\frac{1}{E^{h_j}_{\beta_0}-E^{h_j}_{\beta_1}+\hbar\omega+i\hbar\gamma^{h_j}_{\beta_1}}\right|^2. \quad (11)$$

In deriving Eq. (9), we assume that the inverse lifetime of the electron states is independent of the quantum number m.

The systems under experimental study contain a large number of QD's with different orientations of the crystallographic axes. As a rule, dielectric matrices with built-in nanocrystals can be considered as randomly oriented systems. In this case, of interest is the electron-hole pair generation rate averaged over the orientation of the QD, or over polarization of the light wave,

$$\overline{W^{(2)}}=\frac{16\pi P^2}{9\hbar}\left(\frac{eA}{c}\right)^4\sum_{j=1}^{3}F_{c,h_j}. \quad (12)$$

The important feature of the given two-photon transitions are the selection rules, different from those for the one-photon transitions.[5] According to Eqs. (8) and (10), it is possible to generate only such electron-hole pairs for which quantum numbers of the electron (l_1, m_1) and hole (l_0, m_0) satisfy the relations $\Delta l=l_1-l_0=\pm1$ and $\Delta m=m_1-m_0=0,\pm1$.

The expressions for the TPGR, Eqs. (9) and (12), are applicable to semiconductors of O_h and T_d symmetries. However, in the materials of the second type there is another important channel of two-photon transitions, with the same selection rules as for one-photon transitions. This channel describes transitions for which the intermediate states are bands different from c and h_j bands, and exists due to the fact that, in noncentrosymmetric (e.g., T_d) semiconductors, two-photon transitions are allowed in the dipole approximation. It is well known[6] that the effective-mass approximation is based on the premise that the bands taken into account explicitly (in our case c and h_j) are separated from the others by fairly wide energy gaps ΔE. The criterion for the effective-mass approximation to be applicable in describing two-photon transitions is the inequality $2\hbar\omega\ll\Delta E$. This inequality permits the matrix element (2) to be represented as a product of ω-independent constants and quadratic combinations of the Cartesian components of the vector potential. For the T_d group only one such constant Q is nonzero. Therefore, the matrix elements (2) take a form similar to Eq. (5),

$$\langle c,b'|M|h,b\rangle=-i\delta_{n',n}\delta_{l',l}\delta_{m',m}\frac{Q}{\sqrt{3}}\left(\frac{eA}{\hbar c}\right)^2\begin{pmatrix}\sqrt{3}\epsilon_{0-1} & 0 & i\sqrt{2}\epsilon_{xy} & -\epsilon_{0+1} & -i\epsilon_{xy} & \sqrt{2}\epsilon_{0+1}\\ 0 & -\sqrt{3}\epsilon_{0+1} & \epsilon_{0-1} & i\sqrt{2}\epsilon_{xy} & \sqrt{2}\epsilon_{0-1} & i\epsilon_{xy}\end{pmatrix}, \quad (13)$$

where $\epsilon_{ij}=e_ie_j$. Then, the TPGR in a QD is easily obtained:

$$W^{(2)}_{T_d}=\frac{2\pi Q^2}{3\hbar}\left(\frac{eA}{c\hbar}\right)^4[3(\epsilon_{zz}-\epsilon^2_{zz})\Phi_{c,h_1}+(4\epsilon^2_{xy}+\epsilon_{zz}-\epsilon^2_{zz})\Phi_{c,h_2}+2(\epsilon^2_{xy}+\epsilon_{zz}-\epsilon^2_{zz})\Phi_{c,h_3}], \quad (14)$$

where

$$\Phi_{c,h_j}=\sum_{\beta_0}(2l_0+1)\delta(E^c_{\beta_0}-E^{h_j}_{\beta_0}-2\hbar\omega). \quad (15)$$

The dipole-allowed TPGR averaged over orientation of the QD takes the form

$$\overline{W^{(2)}_{T_d}}=\frac{4\pi Q^2}{15\hbar}\left(\frac{eA}{c\hbar}\right)^4\sum_{j=1}^{3}\Phi_{c,h_j}. \quad (16)$$

From Eqs. (14)–(16) it follows that this channel of two-photon transitions satisfies the selection rules coinciding with the ones for one-photon transitions,[5] i.e., $n_1=n_0$, $l_1=l_0$, and $m_1=m_0$.

As a result of size-quantization effect, the TPGR, $W^{(2)}$, and $W^{(2)}_{T_d}$ possess line energy spectra that are superpositions of contributions of transitions from three valence bands to the conduction band [Eqs. (9) and (14)]. Note that the positions of the lines in the $W^{(2)}_{T_d}$ spectrum and in the spectrum of the one-photon electron-hole pair generation rate $W^{(1)}$ coincide with each other, since the latter rate is determined by the same form functions $\Phi_{c,h}$ from Eq. (15) as the two-photon rate $W^{(2)}_{T_d}$, if $2\hbar\omega$ in Eq. (14) is substituted with $\hbar\omega$.

Figures 1–3 show the low-energy spectra of the form functions $\Phi_{c,h}$ (a) and $F_{c,h}$ (b) calculated from Eqs. (10) and (15) for the three values of the QD radius, $R=1.6$, 2.0, and 2.5 nm. In this energy range the confinement-induced peculiarities in the optical spectra of the QD are most pronounced and an important nonlinear effect such as the double optical resonance can be neglected.[8] Hereinafter calculations are carried out for a cubic CdS crystal with the following parameters: $\Delta_{so}=0.075$ eV, $E_{h_1}=2.42$ eV,[9] $m_c=0.205m_0$, $m_{h_1}=1.348m_0$, $m_{h_2}=0.192m_0$, $m_{h_3}=0.33m_0$,[1] and $\gamma=\gamma^a_\beta=0.06$ eV.[10]

The $\Phi_{c,h}$ and $F_{c,h}$ spectra show some similarities along with essential differences. On one hand, all spectra exhibit a low-energy threshold which shifts to higher energies with decreasing QD radius. As this takes place, the energy density of lines, or the number of lines per a given energy range, decreases. On the other hand, due to different selection rules, the positions of lines in the $\Phi_{c,h}$ and $F_{c,h}$ spectra do not coincide. In particular, the threshold in the $F_{c,h}$ spectrum occurs at a higher energy than in the $\Phi_{c,h}$ spectrum. The behavior of the line amplitudes in relation to the QD radius is also different for $\Phi_{c,h}$ and $F_{c,h}$. The $\Phi_{c,h}$ amplitudes are independent of R and determined by the value of $2l_0+1$

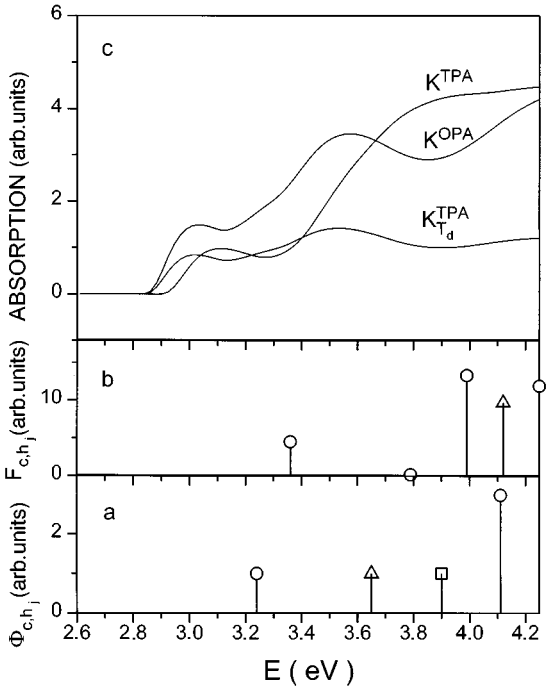

FIG. 1. (a) and (b) Calculated spectra of the form functions Φ_{c,h_j} (a) and F_{c,h_j} (b) for a QD of cubic CdS with a radius $R=1.6$ nm. Circles, triangles, and squares correspond to transitions from the valence bands h_1, h_2, and h_3 to the conduction band c, respectively. (c) Calculated absorption spectra, K^{TPA}, $K^{\mathrm{TPA}}_{T_d}$, and K^{OPA}, for a system of QD's with a size distribution described by Eq. (18), an average radius $R_0=1.6$ nm, and the concentration $N=$ const. See text for the material parameters used in the calculations. $E=\hbar\omega$ for Φ_{c,h_j} and K^{OPA}; $E=2\hbar\omega$ for F_{c,h_j}, K^{TPA}, and $K^{\mathrm{TPA}}_{T_d}$.

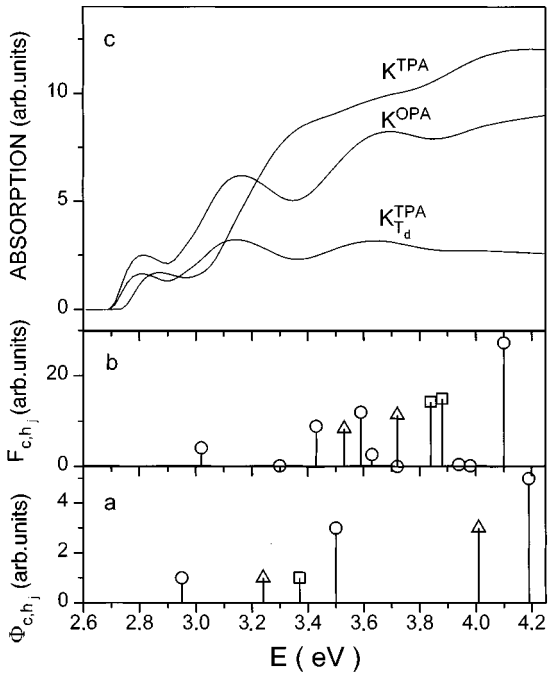

FIG. 2. (a)–(c) Same as Figs. 1(a)–1(c), but for $R=R_0=2.0$ nm.

only, while the $F_{c,h}$ amplitudes are complicated functions of R. The dependence of these functions on R is illustrated in Fig. 4, where the line amplitude for the transition $|h_1,1,1\rangle\rightarrow|c,1,0\rangle$ is shown. Hereinafter the second and third indexes in the ket correspond to the value of n and l, respectively. For a cubic CdS crystal with the above-listed parameters, this transition is the lowest in energy. The shape of the curve in Fig. 4 is defined by two factors: the factor R^{-2} connected with the intraband matrix element [Eq. (6)], and the dependence of the energy denominators in Eq. (11) on R.

Another important difference of $W^{(2)}$ from $W^{(2)}_{T_d}$ and $W^{(1)}$ is its complicated dependence on the effective masses of carriers. As follows from Eq. (15), the effective masses control only the spectral positions of the lines for $W^{(2)}_{T_d}$ and $W^{(1)}$. In this case, the rates $W^{(2)}_{T_d}$ and $W^{(1)}$ depend on the reduced electron and hole masses, $\mu_h=m_c m_h/(m_c+m_h)$. With decreasing μ_h the contribution from the h band to the total spectrum is shifted to higher energies, while the sequence of lines related to this band remains unchanged. The rate $W^{(2)}$ depends on individual values of m_c and m_h. In this case, besides the higher-energy shift of the spectrum as a whole, with decreasing m_c or m_h the sequence of lines controlled by the ratio m_h/m_c may be changed. For instance, if $m_h/m_c=1$, each line is a ''doublet.'' In contrast to the $W^{(2)}_{T_d}$ and $W^{(1)}$, the amplitudes of the $W^{(2)}$ lines depend on the effective masses of carriers.

III. TWO-PHOTON INTERBAND ABSORPTION COEFFICIENT

Using the results derived in Sec. II, the two-photon absorption coefficient for a medium with nanocrystals can be

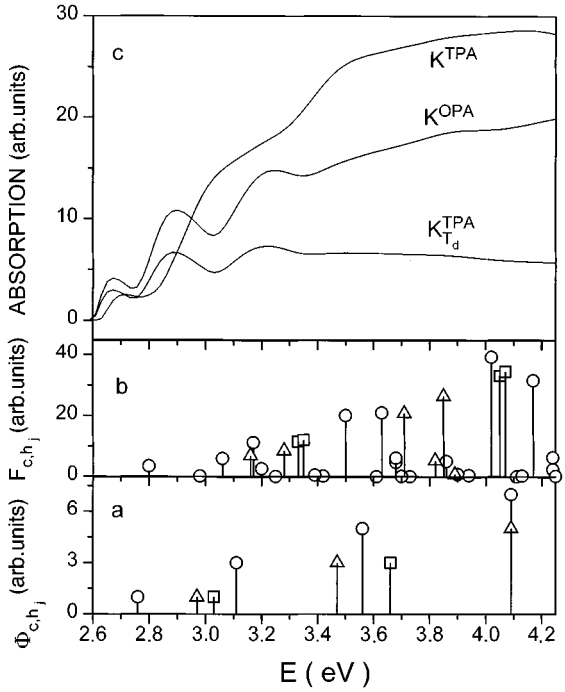

FIG. 3. (a)–(c) Same as Figs. 1(a)–1(c), but for $R=R_0=2.5$ nm.

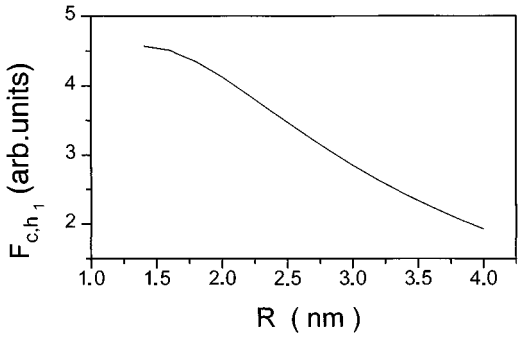

FIG. 4. Size dependence of the line amplitude corresponding to the lowest two-photon transition $|h_1,1,1\rangle \rightarrow |c,1,0\rangle$ in a QD of cubic CdS.

easily calculated if the size-uniform dots are oriented in the same direction [Eqs. (9) and (14)] or randomly [Eqs. (12) and (16)]. To do this, it will suffice to multiply the corresponding expression for the TPGR by the energy absorbed in one transition $2\hbar\omega$, and the QD concentration N, and to divide by the light intensity $I=\varepsilon_\omega^{1/2}\omega^2A^2(2\pi c)^{-1}$, where ε_ω is the dielectric constant of semiconductor at the light frequency. However, in the samples available for experimental studies, the system of randomly oriented nanocrystals exhibits a size dispersion, which can be characterized by a size-distribution function $f(R)$. Hence, to obtain the two-photon absorption coefficient for a given QD system, the size-averaged TPGR should be calculated,

$$K^{\mathrm{TPA}}=2\hbar\omega\frac{N}{I}\int dRf(R)\overline{W^{(2)}}. \tag{17}$$

The question about the distribution function $f(R)$ is of interest in itself, but its discussion in detail is beyond the scope of this work. Note, however, that the main factor responsible for the shape of $f(R)$ is the conditions of sample preparation. Currently, the Gaussian function or the Lifshits-Slezov distribution[11] are mostly used as $f(R)$ functions. The latter distribution

$$f(R)=\begin{cases}\dfrac{3^4}{2^{5/3}}\dfrac{\mathcal{R}^2}{R_0}\dfrac{\exp[1-1/(1-2\mathcal{R}/3)]}{(\mathcal{R}+3)^{7/3}(\frac{3}{2}-\mathcal{R})^{11/3}}, & \mathcal{R}<\frac{3}{2},\\ 0, & \mathcal{R}>3/2,\end{cases} \tag{18}$$

with $\mathcal{R}=R/R_0$ is characterized by a single parameter, the average QD radius R_0.

An important feature of the results of Sec. II is the possibility of calculating the two-photon absorption coefficient in an explicit form with an arbitrary function $f(R)$. Indeed, substituting Eqs. (12) and (16) into Eq. (17), and using the properties of the δ function, we readily obtain

$$K^{\mathrm{TPA}}=\frac{2\pi\omega NI}{\varepsilon_\omega}\left(\frac{8\pi e^2P}{3c\omega^2}\right)^2\sum_{j=1}^{3}\langle F_{c,h_j}\rangle, \tag{19}$$

$$K_{T_d}^{\mathrm{TPA}}=\frac{2\pi\omega NI}{15\varepsilon_\omega}\left(\frac{4\pi e^2Q}{\hbar^2c\omega^2}\right)^2\sum_{j=1}^{3}\langle\Phi_{c,h_j}\rangle, \tag{20}$$

where the average form functions of two-photon transitions are as follows:

$$\langle F_{c,h_j}\rangle=\frac{1}{2\Delta_{h_j}}\sum_{\beta_1,\beta_0}(l_1\delta_{l_1,l_0+1}+l_0\delta_{l_1,l_0+1})\times T_{\beta_1;\beta_0}^{c,h_j}\frac{\xi_{\beta_1}^2\xi_{\beta_0}^2}{(\xi_{\beta_1}^2-\xi_{\beta_0}^2)^2}\frac{f(R_{\beta_1;\beta_0}^{(h_j)})}{R_{\beta_1;\beta_0}^{(h_j)}}, \tag{21}$$

$$\langle\Phi_{c,h_j}\rangle=\frac{1}{2\Delta_{h_j}}\sum_{\beta_0}(2l_0+1)R_{\beta_0;\beta_0}^{(h_j)}f(R_{\beta_0;\beta_0}^{(h_j)}). \tag{22}$$

In Eqs. (21) and (22) we have introduced the transition radius

$$R_{\beta_1;\beta_0}^{(h_j)}=\left[\frac{\hbar^2}{2\Delta_{h_j}}\left(\frac{\xi_{\beta_1}^2}{m_c}+\frac{\xi_{\beta_0}^2}{m_{h_j}}\right)\right]^{1/2} \tag{23}$$

and the parameter $\Delta_{h_j}=2\hbar\omega-E_{h_j}$.

Figures 1(c)–3(c) show the calculated two-photon absorption spectra K^{TPA} and $K_{T_d}^{\mathrm{TPA}}$, of the QD with the Lifshits-Slezov size distribution [Eq. (18)] for the average radii $R_0=1.6$, 2.0, and 2.5 nm. The one-photon absorption spectra K^{OPA} are also shown in Figs. 1(c)–3(c) for comparison. The latter spectra, to an accuracy of a constant, are described by Eq. (20), where the form functions of transitions correspond to the rate $W^{(1)}$ and the frequency factor ω^{-3} is replaced by ω^{-1}. An important feature of the distribution described by Eq. (18) is its high asymmetry. As noted in Ref. 5, asymmetry leads to different positions of the maxima in the absorption spectra and of the related lines in the $W^{(1)}$, $W^{(2)}$, and $W_{T_d}^{(2)}$ spectra (Figs. 1–3). In this connection, information about the size distribution of the QD's is very important in analyzing experimental data.

As is evident from the figures, additional information about the energy spectrum of the 3D-confined states can be extracted only if the channel $W^{(2)}$ dominates in two-photon absorption. Since the K^{TPA} spectrum at higher energies is formed by a large number of two-photon transitions, hardly resolvable spectroscopically even if $R_0=$ 2.0 nm, unambiguous information is obtained by the exciting of the lowest two-photon transition $|h_1,1,1\rangle \rightarrow |c,1,0\rangle$.

IV. DISCUSSION

As shown in Sec. II, a very important consequence of 3D confinement is an essential modification of the intraband matrix elements of electron-photon interaction in the QD as compared to bulk materials. From Eqs. (6) and (7) it follows that the intraband matrix element of the electron momentum, $p_{a,b';a,b}=\hbar|V_{b';b}^{(p)}|m_0/m_a$, is inversely proportional to the QD radius R. This size dependence is responsible for changes in the role of interband and intraband optical transitions in multiphoton processes. While for bulk materials the relation $p_{c,h}\gg p_{a,b';a,b}$ is valid, for a QD this inequality is not only weakened but even may be changed to the opposite one, depending on R. The critical value, $R=R_*^{(a)}$, such that $p_{c,h}=p_{a,b';a,b}$, can be estimated by using the well-known formula[12]

$$p_{c,h}=\left[\frac{3}{2}m_0\left(\frac{m_0}{m_c}-1\right)\frac{E_g(E_g+\Delta_{\mathrm{so}})}{3E_g+2\Delta_{\mathrm{so}}}\right]^{1/2}. \tag{24}$$

For cubic CdS crystal the $p_{c,h} \approx 8.8 \times 10^{-20} CGS$ follows from Eq. (24). If the intraband matrix elements between states with $n'=1$, $l'=1$, $m'=0$ and $n=1$, $l=0$, $m=0$ are chosen as characteristic ones, then the critical radius for four bands are equal $R_*^{(c)}=1.1$ nm, $R_*^{(h_1)}=0.16$ nm, $R_*^{(h_2)}=1.14$ nm, and $R_*^{(h_3)}=0.66$ nm. Thus, in the strong confinement regime, the interband matrix elements are still larger than the intraband once the above-mentioned inequality is replaced by a weak inequality for $p_{c,b';c,b}$ and $p_{h_2,b';h_2,b}$. This effect can be manifested more clearly in the InSb or InAs QD systems. Actually, similar estimates of the critical radius, e.g., for the conduction band, show that $R_*^{(c)}=10.24$ and 6.54 nm for these semiconductors, respectively. In the sufficiently small InSb or InAs QD, multiphoton processes will be controlled by channels with a minimal number of interband matrix elements of the momentum and a maximal number of intraband ones. This situation is directly opposed to that for bulk semiconductors under interaction with plane-polarized light, and should be considered as a very important feature of 3D-confined systems. In this connection, experimental studies of multiquantum processes, such as multiphoton absorption, resonant hyper-Raman and hyper-Rayleigh scattering, etc., in InSb and InAs QD's are of great interest.

As shown above for QD's of T_d semiconductors, there exist two competitive channels of two-photon transitions with different light polarization dependences and selection rules. The latter leads to different spectral positions of absorption peaks for the channels [Figs. 1(c)–3(c)]. To distinguish between the channels of two-photon transitions, we could compare the experimental spectra of one- and two-photon absorption; however, a precise determination of peak positions in the corresponding spectra is usually hampered by the large homogeneous and inhomogeneous broadening. At the same time, different size dependences of K^{TPA} and $K_{T_d}^{\mathrm{TPA}}$ allow us to find the dominant mechanism of two-photon transitions. According to Eq. (20), the ratio $K_{T_d}^{\mathrm{TPA}}(\omega)/K^{\mathrm{OPA}}(2\omega)$ equals the size-independent constant $(4\pi/5)(Q/P)^2 e^2 I/(\omega^2 \varepsilon_\omega^{1/2} \hbar^2 c)$, whereas $K^{\mathrm{TPA}}(\omega)/K^{\mathrm{OPA}}(2\omega)$ increases with the decreasing average radius of the QD. Consequently, the main channel of the two-photon transition and the constant Q could be determined from the size dependence of two- and one-photon absorption coefficient ratios at fixed I and ω.

It should be emphasized that only one channel of two-photon transitions exists in the QD of O_h semiconductors. Since the selection rules for these transitions and one-photon transitions differ, the more pronounced distinctions in the peak positions of one- and two-photon absorption spectra will be manifested as compared with the QD's of T_d semiconductors.

The lack of experimental data on two-photon transitions in QD's of cubic semiconductors at strong confinement do not allow us to compare our results with experimental ones in detail. The experimental two-photon absorption spectra have been observed only for the QD's based on hexagonal CdS.[1] In that work, the energies of two-photon absorption peaks coincided with those of the one-photon absorption spectra; this fact was interpreted as a result of the valence-band mixing. Let us briefly consider Ref. 1 in the light of our results. Both channels of two-photon transitions discussed above exist in hexagonal crystals. In addition, a third channel of two-photon transitions with the same selection rules as one-photon ones exists for C_{6v} semiconductors. This channel is related to dipole-allowed two-photon transitions involving states from c and h_j bands, and thus it cannot be described by the ω-independent constant Q. The competition of the three types of two-photon transitions in combination with a very complicated band structure and large homogeneous and inhomogeneous broadening leads to the conclusion that spectroscopy of two-photon absorption has little promise for a study of QD's of C_{6v} semiconductors. It is possible that, for these reasons, a spectral shift between the peak positions of one- and two-photon absorption for the QD of hexagonal CdS has not been found.[1] We hope that a completely different situation will occur in QD's of cubic semiconductors due to the fairly simple structure of energy bands and the existence of only two-photon transitions or even one channel of two-photon transitions. Consequently, an experimental study of two-photon absorption as well as other multiphoton effects is of great interest in such systems.

ACKNOWLEDGMENTS

Two of us (A.V.F. and A.V.B.) are grateful to the Russian Basic Research Foundation (RBRF), Grants Nos. 96-02-16235a, 96-0216242a, and 95-02-03821a, for financial support of this work.

[1] K. I. Kang, B. P. McGinnes, Sandalphon, Y. Z. Hu, S. W. Koch, N. Peyghambarian, A. Mysyrowicz, L. C. Liu, and S. H. Risbod, Phys. Rev. B **45**, 3465 (1992).

[2] A. P. Alivisatos, A. L. Harris, N. J. Levinos, M. L. Steigerwalg, and L. E. Brus, J. Chem. Phys. **88**, 4001 (1988); D. J. Norris, A. Sacra, C. B. Murray, and M. G. Bawendi, Phys. Rev. Lett. **72**, 2612 (1994); S. V. Gaponenko, U. Woggon, A. Uhrig, W. Langbein, and C. Klingshirn, J. Lumin. **60-61**, 302 (1994).

[3] D. W. Hall and N. F. Borrelli, J. Opt. Soc. Am. B **5**, 1650 (1988); T. Kataoka, T. Tokizaki, and A. Nakamura, Phys. Rev. B **48**, 2815 (1993).

[4] A. V. Baranov, K. Inoue, K. Toba, A. Yamanaka, V. I. Petrov, and A. V. Fedorov, Phys. Rev. B **53**, 1721 (1996).

[5] Al. L. Efros and A. L. Efros, Fiz. Tekh. Poluprovodn. **16**, 1209 (1982) [Sov. Phys. Semicond. **16**, 772 (1982)]; E. Hanamura, Phys. Rev. B **37**, 1273 (1988).

[6] G. L. Bir and G. E. Pikus, *Symmetry and Strain-Induced Effects in Semiconductors* (Wiley, New York, 1975).

[7] H. A. Bethe, *Intermediate Quantum Mechanics* (Benjamin, New York, 1964).

[8] E. Yu. Perlin and A.V. Fedorov, Opt. Spektrosk. **78**, 445 (1995).

[9] A. D. Yoffe, Adv. Phys. **42**, 173 (1993).

[10] U. Woggon, S. V. Gaponenko, A. Uhrig, W. Langbein, and C. Klingshirn, Adv. Mater. Opt. Electron. **3**, 141 (1994).

[11] I. M. Lifshitz and V. V. Slezov, Zh. Éksp. Teor. Fiz **35**, 479 (1958) [Sov. Phys. JETP **8**, 331 (1959)].

[12] O. Madelung, *Physics of III-V Compounds* (Wiley, New York, 1964).